Tunable, continuous-wave single-resonant optical parametric oscillator with output coupling for resonant wave

2016 Chinese Phys. B 25 014208

(http://iopscience.iop.org/1674-1056/25/1/014208)

Tunable, continuous-wave single-resonant optical parametric oscillator with output coupling for resonant wave*

Xiong-Hua Zheng(郑雄桦), Bao-Fu Zhang(张宝夫), Zhong-Xing Jiao(焦中兴)†, and Biao Wang(王彪)‡

The School of Physics and Engineering, Sun Yat-sen University, Guangzhou 510275, China

(Received 4 June 2015; revised manuscript received 25 July 2015; published online 30 November 2015)

We present a continuous-wave singly-resonant optical parametric oscillator with 1.5% output coupling of the resonant signal wave, based on an angle-polished MgO-doped periodically poled lithium niobate (MgO:PPLN), pumped by a commercial Nd:YVO_4 laser at 1064 nm. The output-coupled optical parametric oscillator delivers a maximum total output power of 4.19 W with 42.8% extraction efficiency, across a tuning range of 1717 nm in the near- and mid-infrared region. This indicates improvements of 1.87 W in output power, 19.1% in extraction efficiency and 213 nm in tuning range extension in comparison with the optical parametric oscillator with no output coupling, while at the expense of increasing the oscillation threshold by a factor of ~ 2. Moreover, it is confirmed that the finite output coupling also contributes to the reduction of the thermal effects in crystal.

Keywords: continuous wave, frequency conversion, optical parametric oscillators, output coupling

PACS: 42.65.Yj, 42.70.Mp, 42.60.Lh **DOI:** 10.1088/1674-1056/25/1/014208

1. Introduction

High-power, continuous-wave (cw) optical parametric oscillators (OPOs) are excellent coherent light sources for various applications including trace gas detection,[1,2] high-resolution molecular spectroscopy[3,4] and optical radiometry,[5] which require a combination of high spectral resolution and broadband wavelength tunability in the important infrared (IR) spectral region of 1–4 μm wavelength. Although doubly and triply resonant OPOs can be operated with lower pump threshold (1–100 mW), singly resonant OPOs (SROs) have been more widely used as infrared sources because of their advantageous conversion efficiency, stability and tuning properties.

With the development of periodically poled crystals as parametric materials and high power diode-pumped solid-state laser (DPSSL) or fiber laser as pump sources, various cw SROs with high performance in efficiency, stability, tunability and other characteristics have been demonstrated.[6–8] In a typical SRO, the cavity loss of the resonant signal wave is considered to be as low as possible to minimize the threshold, while maximum output coupling for the non-resonant idler wave is provided to ensure the singly resonating and achieve highest power extraction. In these cases, however, the signal wave is inaccessible. To extract the resonant signal wave, with nonlinear crystals such as PPLN that possesses a large effective nonlinear coefficient, conditions can be somewhat relaxed and finitely coupling out the signal is tolerated.[9,10] Recently, Li *et al*. obtained 6.2 W of signal at 1.56 μm at an extraction efficiency of 42.8% from a double-pass-pumping SRO by employing a 2.5% output coupler.[11] The finite output coupling of the resonant signal wave not only increases the extraction efficiency in the near-IR, but also greatly reduces the intracavity intensity, and hence the thermal effects.

Here, we portray a cw SRO with finite signal output coupling, and a typical cw SRO with no output coupling for comparison. Both of them are based on an angle-polished MgO:PPLN in a four-mirror unidirectional ring cavity, providing high conversion efficiency and wide tunability in the near- and mid-IR. Performances of both configurations with regards to oscillation threshold, idler and signal output power, extraction efficiency, and useful tuning range are presented. A comparative analysis of the thermal effects in the MgO:PPLN crystal induced by the absorption of the intense resonant signal wave is also performed.

2. Experimental setup

As depicted in Fig. 1, the SRO in our experiment is pumped by a commercial cw Nd:YVO_4 solid-state laser (Bavarian Photonics, DPSSL-1064-8-V), delivering stable output power up to 9.8 W at 1064 nm with a 0.8-mm diameter in TEM_{00} spatial mode ($M^2 \sim 1.2$). The pump beam is confocally focused to yield a beam waist of $\sim$50 μm inside the crystal by a single lens ($f = 75$ mm), corresponding to a focusing parameter of $\xi_p \sim 1.6$. The optical cavity is a four-mirror bow-

*Project supported by the National Natural Science Foundation of China (Grant Nos. 61308056, 11204044, 11232015, and 11072271), the Research Fund for the Doctoral Program of Higher Education of China (Grant Nos. 20120171110005 and 20130171130003), the Fundamental Research Funds for the Central Universities of China (Grant No. 14lgpy07), and the Opening Project of Science and Technology on Reliability Physics and Application Technology of Electronic Component Laboratory, China (Grant No. ZHD201203).

†Corresponding author. E-mail: jiaozhx@mail.sysu.edu.cn

‡Corresponding author. E-mail: wangbiao@mail.sysu.edu.cn

tie ring configuration, essentially identical to that used in the early work of Bosenberg *et al.*[12] and various others. The cavity comprises two concave mirrors, M_1 and M_2 ($r = 100$ mm), and two plane mirrors, M_3 and M_4. In SRO, all mirrors are highly reflective at the signal wavelength ($R > 99.9\%$) and highly transparent for the pump ($R < 2\%$) and idler ($R < 5\%$), ensuring the pure single resonance inside the cavity. While in output-coupled SRO (OC-SRO), the configuration is identical to the SRO, except for the replacement of mirror M_4 with an output coupler at the signal wavelength ($T \sim 1.5\%$). The nonlinear crystal is a 5% doped MgO:PPLN (HC Photonics Inc.) with a dimension of $50\times8.6\times1$ mm^3, containing 7 separated gratings with poling periods from 28.5 μm to 31.5 μm in steps of 0.5 μm. Both end faces of the crystal are broadband antireflection coated to avoid residual etalons, and one of them is angle-polished (0.7°). The crystal is housed in an oven of which the temperature can be stabilized within ±0.1 °C ranging from room temperature to 200 °C. The resonant signal in the cavity has a beam radius of 72 μm in the center of the crystal, corresponding to a focusing parameter of $\xi_s \sim 1.2$, slightly deviating from ξ_p. A dichroic mirror, M, separates the generated idler output from the residual pump and signal radiation.

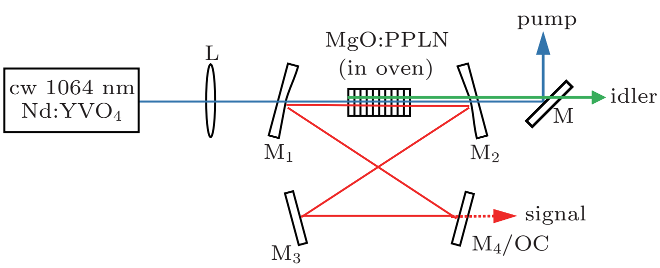

Fig. 1. (color online) Schematic of the cw SRO based on MgO:PPLN in a bow-tie ring cavity. L: lens, M: dichroic mirror, OC: output coupler.

3. Results and discussion

We investigate the power scaling of both configurations for comparison. The measurements are performed at a crystal temperature of 90 °C for the same grating period (Λ = 31.0 μm). For the SRO, as shown in Fig. 2(a), an idler power of 2.05 W is obtained by scaling the pump power up to 9.8 W, indicating an extraction efficiency of 20.9%. In contrast, the measured correlation between extracted power and pump power for OC-SRO is shown in Fig. 2(b). At a maximum pump power of 9.8 W, 1.83 W of idler power is obtained, corresponding to an extraction efficiency of 18.7%. While the 1.5% transmission of the output coupling at the signal wavelength extracts a maximum signal power of 2.25 W, corresponding to an extraction efficiency of 23%. The OC-SRO shows a slight reduction in idler power, but a total extraction efficiency of 41.7% is available, indicating an improvement of 20.8% in comparison with the SRO.

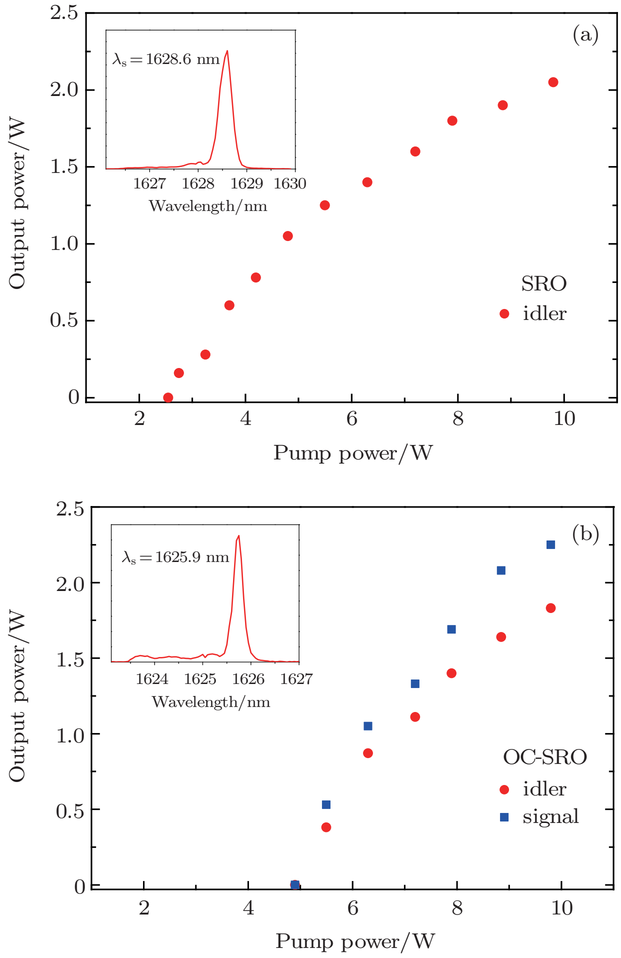

Fig. 2. (color online) Curves of extracted power versus pump power at Λ = 31.0 μm, T = 90 °C for MgO:PPLN in SRO (a) and OC-SRO (b).

Given the threshold of 2.6 W in SRO, the sum of all residual losses for the signal wavelength inside the cavity is estimated to be 1.8% according to Ref. [13]. On the other hand, the threshold of the OC-SRO is 4.9 W. Taking the output coupling loss as 1.5%, the sum of all residual losses is estimated to be 1.9%, which is almost the same as the one in SRO. This is reasonable since the only difference between the two configurations lies in the output coupler. Such a high residual loss for the signal wave is believed to stem from the imperfect coating of the cavity mirrors and crystal end faces, and the crystal absorption as well. The signal wavelength is measured to be 1628.6 nm and 1625.9 nm in the SRO and OC-SRO (shown in the insert of Fig. 2), respectively, implying a temperature deviation of ∼ 3.5 °C in MgO:PPLN, as calculated from the Sellmeier equations.[14] This temperature drop in OC-SRO is mainly attributed to the output coupling of resonant signal, which greatly reduces the crystal absorption of signal power.

Broadband tunability is available in both configurations by taking advantage of the multi-period PPLN together with a temperature-controlled oven. By changing the grating period in steps of 0.5 μm, coarse wavelength tuning can be obtained; fine tuning can be achieved by scanning the temperature of the PPLN in small steps. According to the theoretical tuning curves calculated from the Sellmeier equations,[14] when the crystal temperature changes from 30 °C to 170 °C, the tuning ranges of the different grating periods overlap. Therefore, continuous wavelength tuning of the output idler in the mid-IR region can be achieved. Figure 3(a) shows the generated idler power across the tuning range in SRO when the pump source operates at a maximum output power of 9.8 W. The OPO is successfully tuned from 2644 nm to 4148 nm with the idler power above 1 W over more than 80% of the 1504-nm-wide tuning range. The leaked-out signal power is ignored. The maximum idler power of 2.32 W is obtained at 2644 nm (Λ = 31.5 μm, T = 130 °C), indicating an extraction efficiency of 23.7% from pump to idler. The output power of idler versus wavelength shows a tendency of gently ramping down towards longer wavelength, due to the fact that the parametric gain experiences a reduction when tuning away from degeneracy. A distinct drop in the idler power around 2.83 μm is explained by the OH^- absorption in MgO:PPLN, while most power drops above 4 μm are also attributed to the significant idler absorption at longer wavelength in $LiNbO_3$ due to multi-phonon absorption. The cause of power drop at 3.97 μm is unknown and probably due to the thermal effects and absorption loss of PPLN.

In the OC-SRO, output powers of extracted idler wave over the tuning range together with the corresponding signal wave are characterized in Fig. 3(b). Note that unlike the case of SRO where we restored the maximum output power at any operation point of the scan, no realignment is performed during the scan in OC-SRO. This means that the cavity alignment may change when the crystal periods are transformed or the crystal temperature is varied, which is ascribed to the fact that the crystal is 0.7°-wedged polished and the crystal refractive index is temperature dependent. However, the idler power in OC-SRO is qualitatively consistent with the SRO. Both idler power and signal power gently ramp down towards longer wavelength due to the reduction of parametric gain. Power dips at 2.83 μm and ∼4 μm are again observed and result from the crystal absorption. With the 1.5% output coupling at the resonant signal wave in OC-SRO, idler power above 1 W over 80% of the 1388-nm tuning range from 2664 nm to 4052 nm, and signal power above 1 W over 80% of the 329-nm tuning range from 1443 nm to 1772 nm are available. The output coupling leads to an increase of threshold, and hence a partial decrease in idler power. However, signal power up to 2.57 W at 1519 nm is extracted out of the cavity. The maximum total output power and extraction efficiency are now 4.19 W (1.89 W idler at 3110 nm and 2.3 W signal at 1617 nm) and 42.8%, respectively, implying an enhancement of 1.87 W in output power and 19.1% in extraction efficiency.

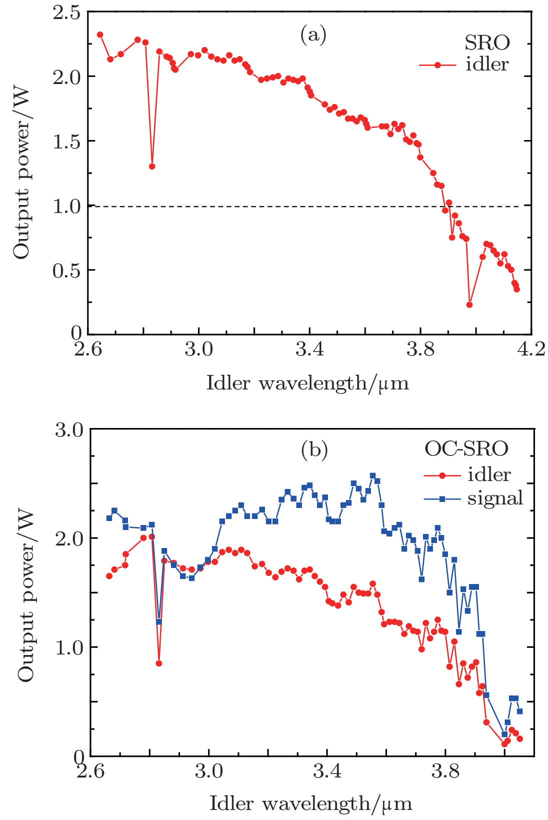

Fig. 3. (color online) Extracted power across the tuning range at a maximum pump power of 9.8 W for (a) SRO, (b) OC-SRO.

It is worth noting that in the SRO configuration, due to the absence of signal output coupling, and hence the critical thermal loading in the crystal, stable operation is unavailable below 35 °C. In contrast, room-temperature operation at 30 °C is possible in OC-SRO configuration, which means that the deployment of output coupling can extend the tuning range of a single period. However, in the case when the OC-SRO is tuned above 4 μm (Λ = 28.5 μm, T < 120 °C), the 1.5% output coupling loss together with the substantial residual loss leads to an unacceptable rise in threshold, rendering OC-SRO operation beyond the reach of our pump source. This accounts for the decreasing of the idler tuning range in OC-SRO. Therefore, an optimal output coupling is desirable, being a trade-off between the extraction power and the rise in threshold. As theoretically predicted, a maximum conversion efficiency is achieved for pumping at $(\pi/2)^2$ times of the oscillation threshold,[15,16] confirming that an output coupling of 1.5% is not optimal for our device and higher output powers in OC-SRO can be expected.

4. Conclusions

In this work, we demonstrate that the OC-SRO configuration shows significant enhancements in extraction efficiency and useful tuning range over SRO with no output coupling, especially in the near-IR region. With finite output coupling of the resonant signal wave, substantial signal power tunable in a wide near-IR region is available for additional applications such as cascaded pumping of mid-IR OPOs, at the expense of increasing the oscillation threshold and slightly decreasing the idler power. In addition, the output coupling also contributes to the reduction of thermal effects in crystal and thus is promising for high-power cw OPOs. Further improvement will be focused on optimizing the output coupling across the tuning range so that higher extracted powers and efficiencies are expected.

References

[1] Cristescu S M, Persijn S T, Hekkert S T L and Harren F J M 2008 *Appl. Phys. B* **92** 343

[2] Ngai A K Y, Persijn S T, Lindsay I D, Kosterev A A, Groß P, Lee C J, Cristescu S M, Tittel F K, Boller K J and Harren F J M 2007 *Appl. Phys. B* **89** 123

[3] Asvany O, Hugo E, Muller F, Kuhnemann F, Schiller S, Tennyson J and Schlemmer S 2007 *J. Chem. Phys.* **127** 154317

[4] Kovalchuk E, Schuldt T and Peters A 2005 *Opt. Lett.* **30** 3141

[5] Lykke K R, Shaw P S, Hanssen L M and Eppeldauer G P 1999 *Metrologia* **36** 141

[6] Lin X C, Bi Y, Yao A Y, Kong Y P, Zhang Y, Sun Z P, Li R N, Cui D F, Xu Z Y and Li J 2003 *Chin. Phys. Lett.* **20** 1074

[7] van Herpen M M J W, Bisson S E, Ngai A K Y and Harren F J M 2004 *Appl. Phys. B* **78** 281

[8] Samanta G K, Fayaz G R and Ebrahim-Zadeh M 2007 *Opt. Lett.* **32** 2623

[9] Samanta G K and Ebrahim-Zadeh M 2008 *Opt. Express* **16** 6883

[10] Kumar S C, Das R, Samanta G K and Ebrahim-Zadeh M 2011 *Appl. Phys. B* **102** 31

[11] Li P, Li Y, Feng J and Zhang K S 2015 *Appl. Opt.* **54** 4374

[12] Bosenberg W R, Myers L E, Byer R L, Drobshoff A and Alexander J A 1996 *Opt. Lett.* **21** 1336

[13] Zeil P, Thilmann N, Pasiskevicius V and Laurell F 2014 *Opt. Express* **22** 29907

[14] Gayer O, Sacks Z, Galun E and Arie A 2008 *Appl. Phys. B* **91** 343

[15] Kreuzer L B 1969 *Proceedings of the Joint Conference on Lasers and Opto-Electronics*, March 25–28, Southampton, England, p. 52

[16] Sowade R, Breunig I, Kiessling J and Buse K 2009 *Appl. Phys. B* **96** 25